Snapshot Hyperspectral Imaging – the Hyperpixel Array™ Camera

Andrew Bodkin, A. Sheinis[1], A. Norton[2], J. Daly, S. Beaven[3] and J. Weinheimer[3]
Bodkin Design & Engineering, LLC, 77 Oak St., Newton, MA 02464
[1]University of Wisconsin-Madison, Dept. of Astronomy, 425 N Charter St., Madison WI 53706
[2]Norton Engineered Optics, 3696 Ross Road, Palo Alto, CA 94303
[3]Space Computer Corporation, 12121 Wilshire Boulevard, Suite 910, Los Angeles, CA 90025

ABSTRACT

Hyperspectral imaging has important benefits in remote sensing and material identification. This paper describes a class of hyperspectral imaging systems which utilize a novel optical processor that provides video-rate hyperspectral datacubes. These systems have no moving parts and do not operate by scanning in either the spatial or spectral dimension. They are capable of recording a full three-dimensional (two spatial, one spectral) hyperspectral datacube with each video frame, ideal for recording data on transient events, or from unstabilized platforms. We will present the results of laboratory and field-tests for several of these imagers operating in the visible, near-infrared, mid-wavelength infrared (MWIR) and long-wavelength infrared (LWIR) regions.

Keywords: Hyperspectral sensor, hyperspectral imaging, HSI, visible, near-infrared, mid-wavelength infrared, long-wavelength infrared, MWIR, LWIR, ruggedized sensor

INTRODUCTION

Hyperspectral imaging has been recognized as an important tool for remote sensing. It can identify materials by the spectral content of a pixel even though the objects of interest are too small to be spatially resolved, are partially obscured by vegetation or can only be identified by their spectral signature. High-spectral-resolution hyperspectral imagery is a key element in the developing fields of autonomous material identification, geological mapping, biological research, medical imaging, cancer detection and clinical instrumentation.

Existing hyperspectral systems typically use one of three techniques: 1) a spatially-scanning slit spectrometer, such as a push-broom imager (AVIRIS[1], HYDICE[2] and SEBASS[3], for example), 2) wavelength tuning a spectral filter, such as a tunable étalon, or Fabry-Pérot filter or 3) scanning the Fourier transform of the spectrum with a two-dimensional (2D) Fourier transform imager. These systems are limited to observing fixed or slow-moving objects because of the need to scan the image. Though such systems have been employed effectively in airborne and satellite applications, they are negatively affected by motion of the platform, motion or changes in the atmosphere and, more importantly, rapid motion, or in the case of the Fourier transform imager, changes of intensity of the objects in the image field. These motions result in mismatched or misaligned sub-images, reducing the utility of the observations. Because of these limitations, traditional hyperspectral systems can not adequately image transient events or operate from handheld or unstabilized vehicle-mounted platforms.

There is a need for a system that can capture both spatial and spectral information simultaneously, without scanning – one that can stare at sources, thereby integrating the

Proc. of SPIE Vol. 7334, Algorithms and Technologies for Multispectral, Hyperspectral, and Ultraspectral Imagery XV, 13 - 17 April 2009, Orlando, Florida, USA

exposure time and enabling the observation of low-light/low-emissivity sources. Such a system can operate in spectral regions previously found to be too low in signal strength for hyperspectral observations. Furthermore, it can measure rapid transient events. Such a device would find wide application in a number of markets by enabling a novel hyperspectral solution. .

Hyperspectral Imaging at the Speed of Light

Bodkin Design & Engineering has developed the HyperPixel Array™ (HPA) Imager. This massively parallel system collects all three dimensions of the full three-dimensional hyperspectral datacube *simultaneously*. Incident photons from an imaged scene are detected in parallel by a two-stage optical processor. This device manipulates the data set prior to any electronic detection or software processing, operating on the data set *at the speed of light*. No computer algorithm can process faster.

Figure 1 shows a fully three-dimensional hyperspectral (two spatial dimensions plus one wavelength dimension) datacube. Wavelength-scanning (tunable filter-type) systems measure a 2D spatial slice at a single wavelength. Slit-scanning (pushbroom) systems measure the spectrum of a one-dimensional (1D) slice of the target scene by dispersing one spatial dimension vs wavelength across the 2D detector array. BD&E's unique HPA system collects the entire datacube simultaneously and distributes the entire cube onto a detector array.

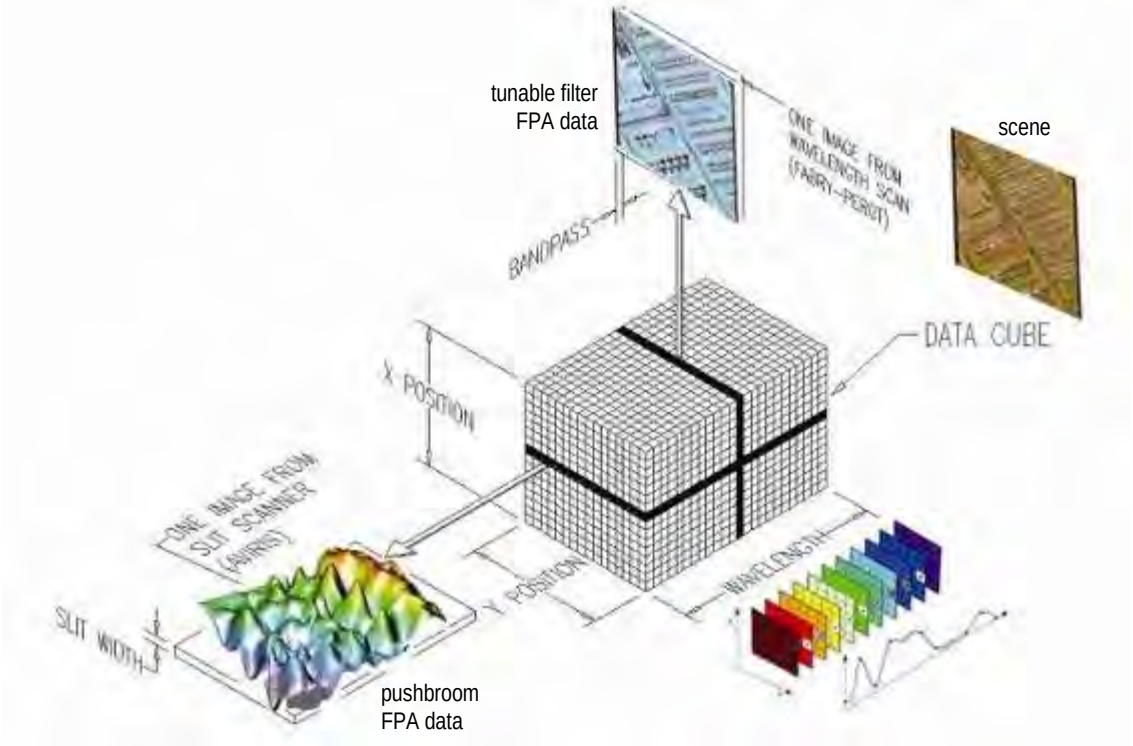

Figure 1. Graphical representation of the 3D hyperspectral datacube and the acquisition parameters of existing systems. Existing scanning systems measure only one slice through the datacube at any given instant. Wavelength-scanning (tunable filter-type) systems measure a slice at a fixed wavelength, slit-scanning (pushbroom) systems measure at a fixed position in one spatial dimension. The HPA system is unique in that a parallel optical processor measures the entire datacube simultaneously, and continuously distributes the entire cube onto a detector array.

The processing system uses a staring array of hyperpixels. Each hyperpixel is a separate spectrographic channel capable of resolving hundreds of spectral bins. Since it is a staring system, its sensitivity can be increased by staring longer and, since it does not scan, there is no temporal distortion of the spatial information.

Optical Processing Techniques

The HPA™ imager uses a pinhole array or short-focal-length, two-dimensional lenslet array located at the image plane of a camera or telescope (foreoptic) to re-sample the scene image and re-image the collecting aperture of the telescope into an array of small sources (pupils) for the spectrometer. A single spectrometer disperses all the pupil images simultaneously. The result of this process is a two-dimensional array of spectra, each from a single spatial element of the image (from a single pinhole or lenslet). These spectra are recorded simultaneously on a two-dimensional detector array (figure 2). Figure 3 shows a section of the first pupil plane and the dispersed spectra on the detector array. Slight rotation of the hyperpixel array relative to the axis of the prism allows spectra to be recorded without interference with each other.

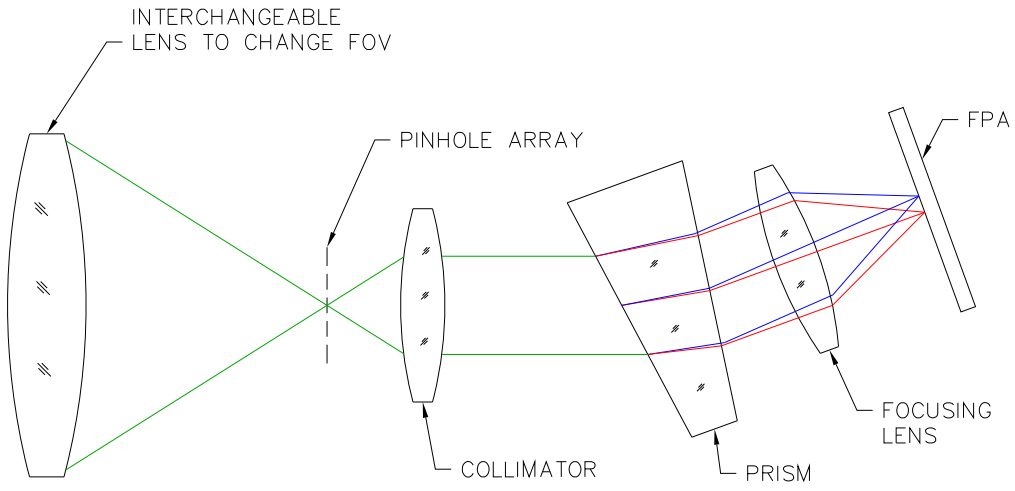

Figure 2. The Hyperpixel Array (HPA) Optical Processor. The input optical element images (focuses) the scene onto a pinhole or lenslet array which spatially samples the scene. The individual scene elements are re-imaged in parallel through a prism onto a conventional focal plane array and read via a frame grabber to a PC. 'Cube formation software' converts the recorded spectra image into a datacube in ENVI format. Standard ENVI software tools can then be employed to process the datacube to produce the required data products. This design allows the entire data cube to be mapped onto the focal plane and to be read out at video frame rates, or faster. The technique has been developed for various wavebands, from the visible through the LWIR.

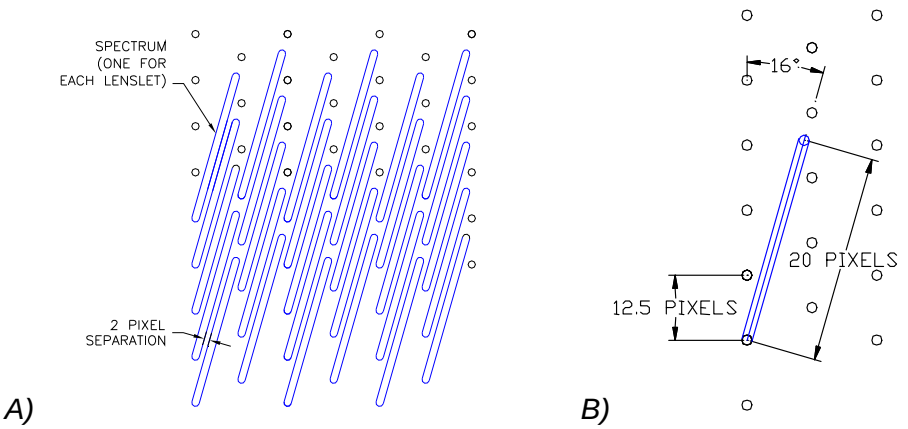

Figure 3. A) Represents the intensity pattern on the CCD. The prism has dispersed each pupil image into its constituent colors. The grid of images in the pupil plane has been rotated by a small angle to assure a separation of at least two detector pixels between adjacent spectra. B) Shows the geometric relationship between the spectra and the array layout. The spectra packing in this example uses a hexagonal lenslet array. Rotating the array 16º permits the spectra to be spread over 20 detector pixels without overlap.

Note that the HPA principle of operation is independent of the choice of focal plane array or wavelength range. The same idea will work for all wavelengths from the UV to the far-IR. Each frame from the FPA provides 3D hyperspectral data. The FPA is read out normally and then the data is re-mapped from 2D, as shown in figure 3A, to a complete 3D hyperspectral datacube (or 'hypercube') similar to that in Figure 1. The dimensions of the hypercube depend on

1. The dimensions of the FPA, *e.g.* 640 pixels × 480 pixels
2. The desired wavelength resolution or number of wavelength channels
3. The pinhole array density (hole spacing)

These can be adjusted during the design phase to achieve a desired hypercube dimension. Trade-offs in this design are: more spectral resolution or more wavelength channels means lower spatial resolution and vice-versa; increasing the pixel count of the FPA while keeping the pinhole count (spatial resolution) constant can increase spectral resolution.

BD&E has been collaborating with Space Computer Corp. (Los Angeles, CA) to develop the FPGA hardware and software algorithms to perform the 2D to 3D re-mapping process in real time. The output will be real-time ENVI™-compatible[4] hyperspectral datacubes with bad pixel and NUC corrections.

SNAPSHOT HYPERSPECTRAL IMAGER

Shown in figure 4 are three prototype HPA™ systems that BD&E has demonstrated for collecting imagery in the Visible/VNIR, MWIR and LWIR spectral regions. Table 1 lists the prototype systems that have been demonstrated by BD&E.

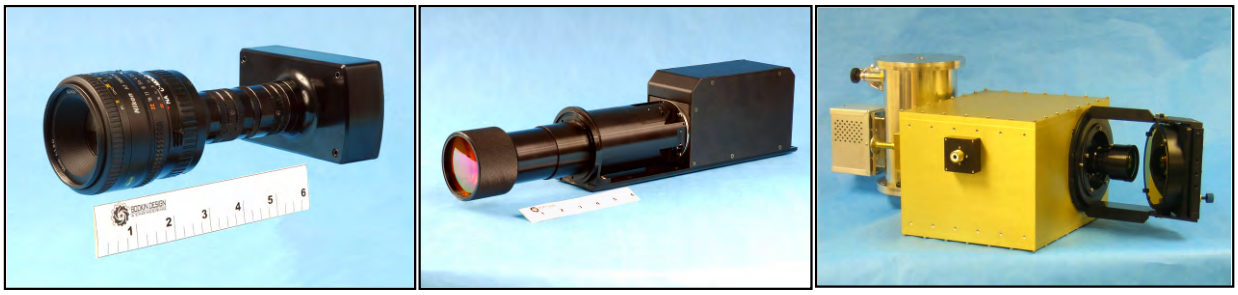

Figure 4. Three prototype HPA™ video systems. The sensors shown from left to right operate in the Visible/VNIR, MWIR and LWIR spectral regions.

Table 1: *Matrix of HyperPixel Array Imagers built by Bodkin Design & Engineering, LLC. The imagers span the visible through LWIR spectral regions with varying spatial and spectral resolution.*

					FOV				
Model	Band (um)	Data Cube H x V x WL	Res. avg. (nm)	IFOV (mrad)	hor (deg)	ver (deg)	f/	frame rate (Hz)	Bit res.
HPA-01	0.45-0.65	57 x 57 x 200	1					15	10
HPA-02	0.42-0.67	180 x 180 x 20	12	1.46	7.6	6.1	1.8	30	10
HPA-03	0.5-0.9	53 x 34 x 106	3.8				4	30	10
HPA-04	0.65-0.87 1.09-1.40	13 x 10 x 450	1.5					29	
HPA-05	3-5	18 x 14 x 59	34	4.66	4.8	3.8	2.5	60	14
HPA-06	7.8-10.8	13 x 10 x 60	50	6.55	7.3	5.5	1.2	30	14

The raw imagery collected from these systems has one spectrum per pinhole on the FPA as shown in figure 5.

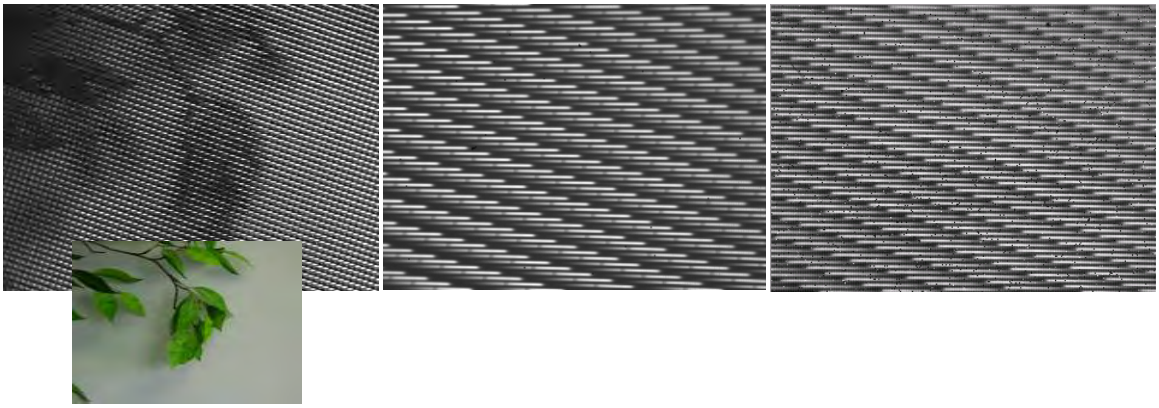

Figure 5. Examples of Raw Imagery of an office plant (inset) from a 20-band visible system (left), a 50-band mid-wavelength infrared system (middle) and a 60-band long-wavelength infrared system (right). Each streak corresponds to a spectrum from a different pinhole. Note that an atmospheric absorption from CO_2 appears as a dark line at 4.2 µm in each of the spectra on the MWIR FPA (center).

Optical design

In the case of the first system built, the visible HPA (figure 4, left), significant modeling was done to evaluate several optical design options for the HPA system. After a trade-off analysis, the design concept in which two fast CCD lenses relay the image onto the CCD array with a zero-deviation prism between them was selected (figure 6). This design has very good spatial resolution because the hyperpixel size is not limited by a fast lenslet size. It also has low stray light, no unwanted orders and no detector window issues, although some vignetting is possible. By using a slightly defocusing fore-optic, the sparse-sampling issue created by the pinholes is eliminated. A ray trace of the instrument built from this design is shown in figure 6. The resulting spot diagram showing the low aberration of this design is shown in figure 7.

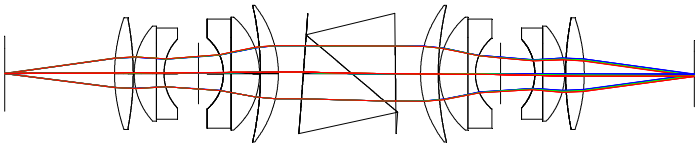

Figure 6. Ray trace of the zero-deviation prism design for the visible HPA system.

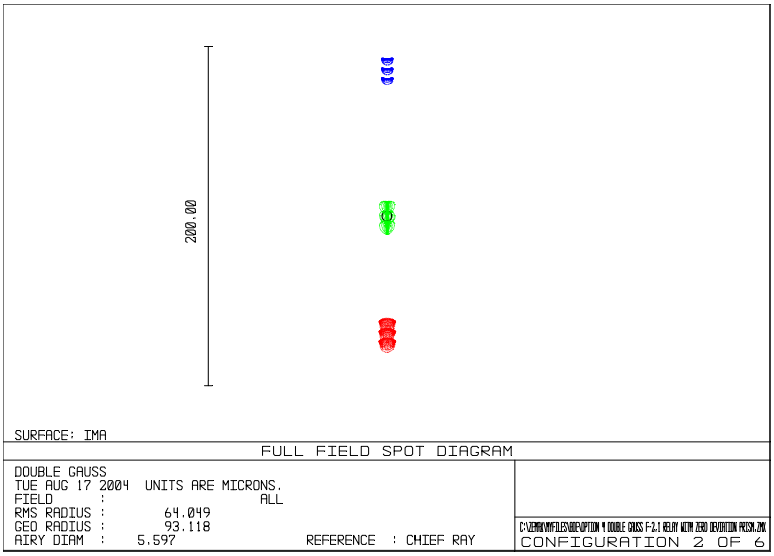

Figure 7. Computed spot diagram of visible HPA system with relay optics and zero-deviation prism. Aberrations such as astigmatism and keystone are small or non-existent.

The zero-deviation prism allowed the system to have a straight optical axis, improving packaging and simplifying construction. It also resulted in spectral dispersion which was more linear over the entire waveband.

The prototype HPA imager based on this design is a compact, robust sensor. The device measures 2.5”W x 4.0”H x 6.9”L and weighs 2 pounds. The optical path, from aperture to FPA, measures a very compact 51mm in length. The device acquires a hyperspectral datacube with 100 x 100 spatial elements by 20 spectral elements. The spectral bandwidth ranges from 425 to 675 nm. The data is acquired at the rate of 15 cubes per second and has an average spectral resolution of 12.5nm/pixel.

This zero-deviation prism design was carried over to system designs for other wavelengths. Different prism materials were selected to be compatible with each system's waveband. For visible through MWIR wavebands, we found that it was not necessary to cool the prisms and other optical components; however, for the LWIR system it was necessary to cool the optics to suppress self-emittance and maintain good signal-to-noise ratios.

Sensor Characterization

The first step in forming hyperspectral datacubes from the raw imagery is to accurately characterize positions of the spectra on the FPA. Monochromatic light (from a blackbody source passed through a monochromator) appears on the FPA as an array of dots identical to the pinhole array. The exact position of the dots depends on wavelength. A series of these monochromatic spot patterns is collected at many wavelengths spanning the spectral range of the instrument in order to determine the FPA x and y positions of these wavelengths for every pinhole. Each resulting spot (excluding bad pixels) is fit with a 2D Gaussian model to provide a more accurate location for the spot center and to characterize the width of the spot in the spectral and cross-spectral directions. Since a fit is made for every spot at each of the monochromatic wavelengths, a map of the fit parameters across the FPA can be generated, which also gives some measure of the uniformity of the dispersion across the FPA. The spots at different wavelengths for the same pinhole are then associated with x and y position on the FPA to provide a description of the spectral response for each pinhole (figure 8).

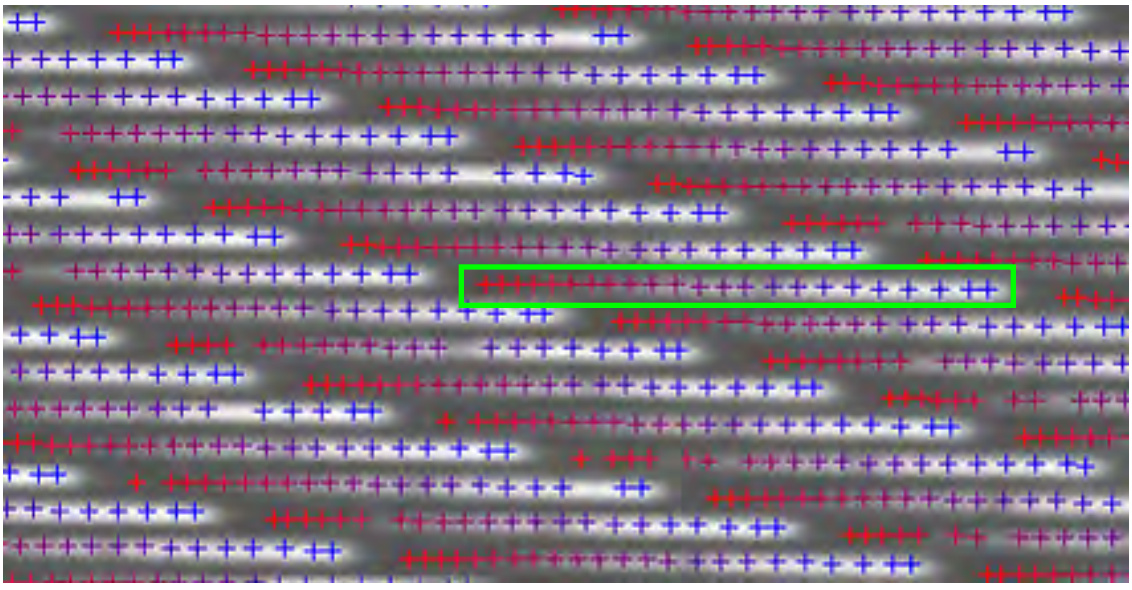

Figure 8. The associated spot positions for each pinhole overlaid on a blackbody spectrum. Each plus sign indicates the position of a monochromator measurement. The color of each plus sign corresponds to its wavelength ranging from blue at 2.9μm to red at 5.1μm. For this particular sensor (MWIR), the spectral direction corresponds to the x direction and the spectra run from low to high wavelengths from right to left. The green box shows the associated position measurements for one of the pinholes.

The associated spot information provides a means to characterize each of the pinhole spectra in terms of wavelength so that the position (and spot width) of any arbitrary wavelength for the pinhole can be found. The accurate description of the pinhole spectra provided by the characterization provides all of the necessary information to extract data from the raw scene imagery and to form spectral datacubes.

Radiometric calibration is performed by having the HPA view a blackbody source at a number of different temperatures. This results in images of spectral 'streaks' with different intensity profiles. By analyzing the images, one can determine radiometric responsivity as well as the pinhole-to-pinhole non-uniformity correction (NUC). This method should yield corrections on approximately the same level of the processed pixel-corrected spectra if the widths of the lines in the cross-spectral direction are sufficiently wide. In the current test instruments, the lines are under-sampled in the cross-spectral direction, so the pixel-level NUC should provide a better NUC over post-NUCing alone.

Hypercube Formation

The information provided by the characterization steps allows us to re-map the 2D spectral 'streaks' in the FPA image into 3D hyperspectral datacubes, to apply a NUC correction, and to calculate source radiance (MWIR and LWIR cameras). Figure 9 presents a block diagram illustrating the strategy for converting arbitrary scene data from acquired with the HPA™ into calibrated 3D hyperspectral datacubes. The NUC coefficients are determined only once, based on blackbody spectra. These are then applied to each subsequent datacube as it is acquired. Figure 10 shows the spectrum for a single pinhole from a datacube formed of a 25°C blackbody after it has been calibrated. This data was acquired with the MWIR HPA™. The measured spectrum shows good agreement with the theoretical blackbody curve. Similarly the visible/NIR HPAs can be calibrated to reflectance units using a dark and white measurement.

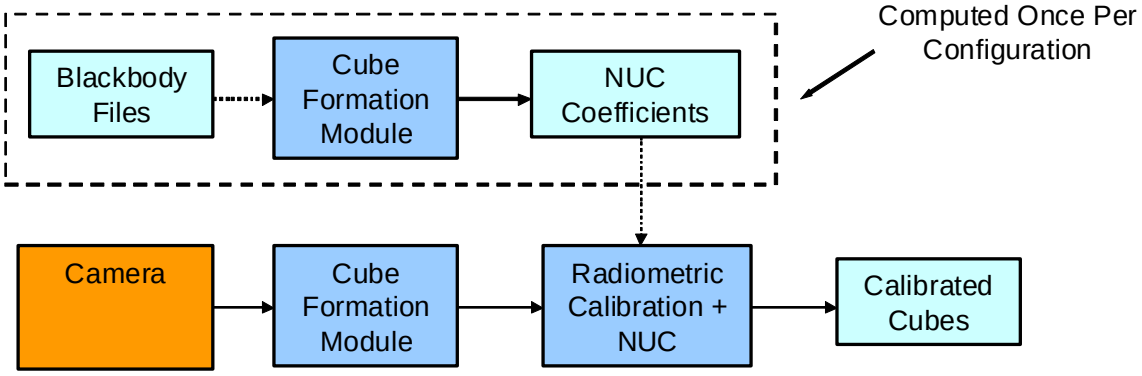

Figure 9. Calibration of formed datacubes. NUC coefficients are computed once per configuration using a set of cubes formed using blackbody curves. These NUC coefficients are then applied to the scene imagery to produce calibrated output cubes.

All of the hypercubes presented in this paper were obtained by post-processing the 2D camera images since the data-processing required is substantial and current laptop computers are not fast enough to perform these operations in real time. However, we recently demonstrated real-time datacube formation at 30Hz for the MWIR HPA™. Space Computer designed, built and tested a custom FPGA processor which remaps the 2D FPA images to 3D datacubes and applies NUC correction. SCC also completed the software and user interface to operate the processor. The details of this effort will be reported at a later date.

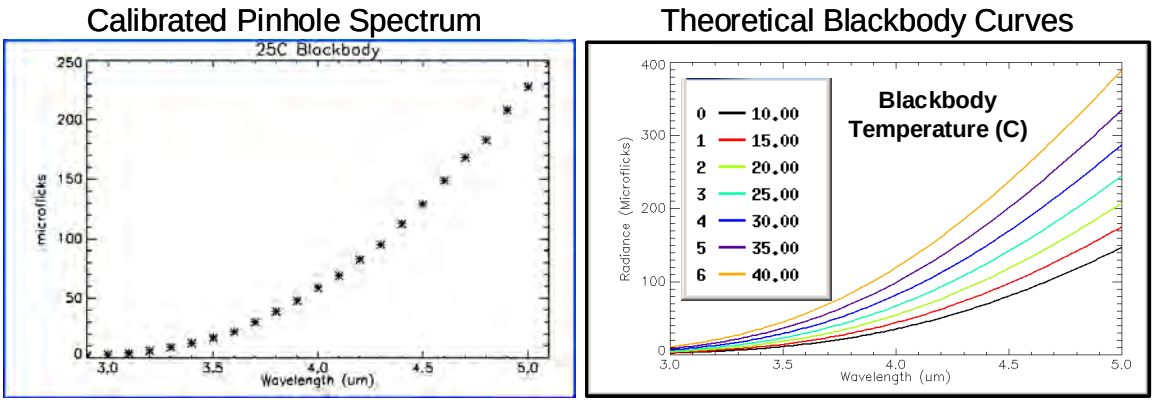

Figure 10. MWIR spectrum from a formed cube for a 25℃ blackbody (left) and the theoretical blackbody curve (right). For the correctly calibrated system, the 25℃ blackbody should be close the theoretical blackbody curve.

Hyperspectral demonstration

To demonstrate the visible HPA™ imager, we acquired hyperspectral images of the BD&E logo under fluorescent light illumination using the visible HPA (figure 11). The data clearly shows the mercury lines from the fluorescent lamp.

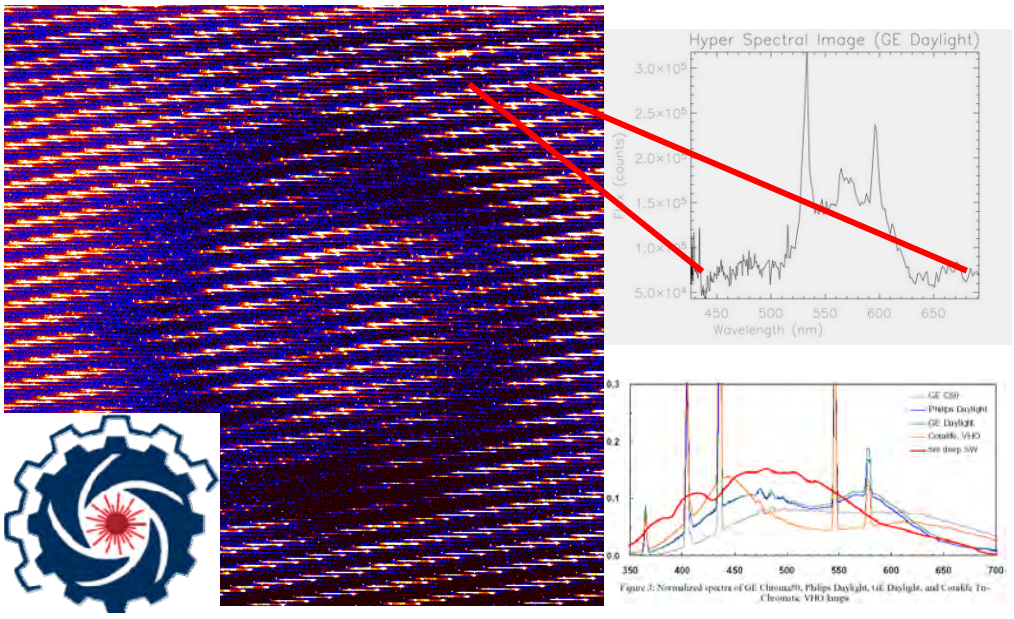

Figure 11. This is a laboratory image of the BD&E logo under fluorescent illumination taken with the Phase I demonstration HPA imager which operates in the visible band. The optically processed image shows the array of dispersed spectral lines. Details of one of the spectral lines is shown in the upper graph; for comparison the lower graph shows several of the spectral lines that are common in fluorescent lighting.

Measurements were also made using the MWIR and LWIR HPA™ imagers. In one test, a road flare was set up at a distance of about 30 feet. The MWIR imager saw only the blackbody radiation (heat) from the flare, but the LWIR imager easily picked up the perchlorate (ClO_4^-) emission at ~9 µm (figure 12).

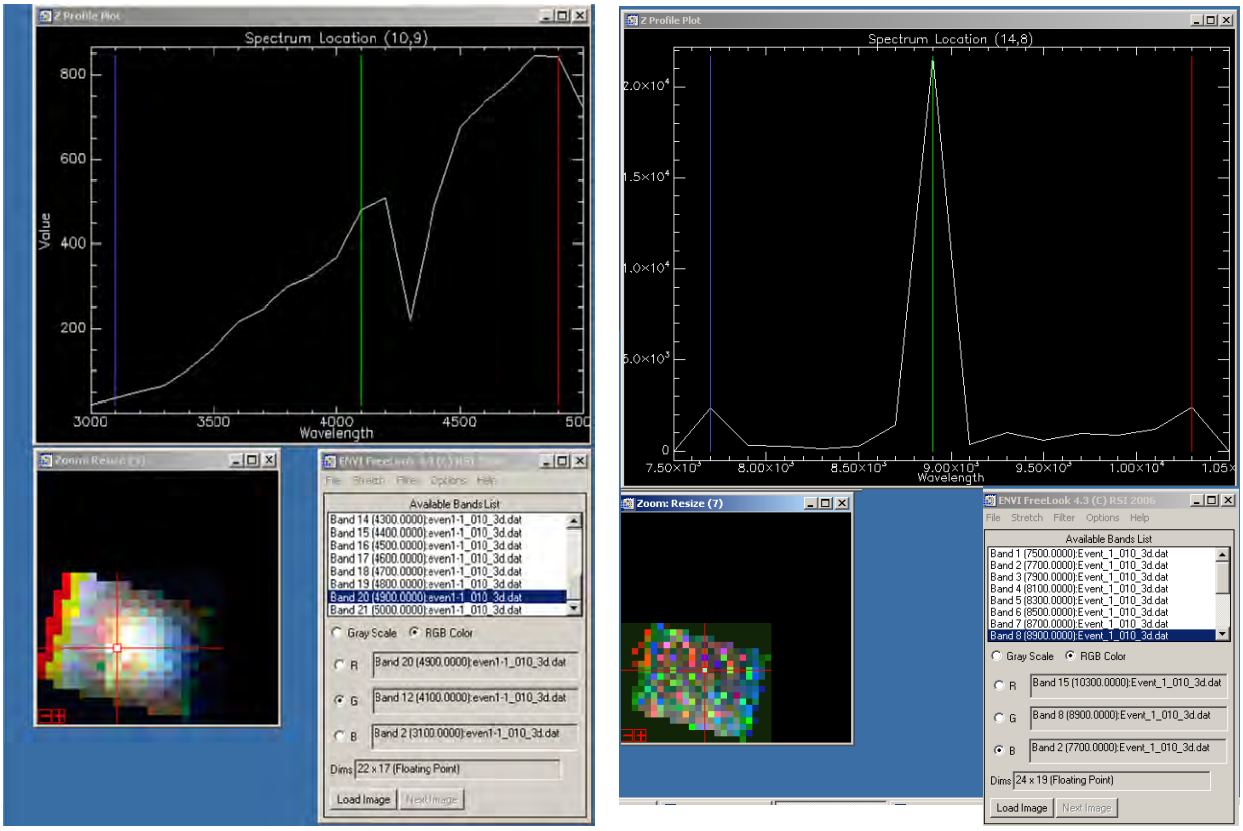

Figure 12. Hyperspectral data acquired while looking at a lit road flare with both the MWIR (left) and LWIR (right) HPA imagers. For each imager, a false (3-)color image of each data cube is shown in the lower left. The top image shows spectral data for the spatial point in the datacube designated by the crosshair. The MWIR imager was able to see only blackbody radiation from the flare as well as atmospheric CO_2 absorption. The LWIR imager was able to clearly pick intense spectral lines near 9 µm. We have identified this as perchlorate, one of the principal ingredients in road flares.

SUMMARY

Bodkin Design and Engineering has developed and demonstrated snapshot hyperspectral imagers in wavebands from the visible through the LWIR. Advantages of the HyperPixel Array™ design include:

1. The HPA™ will reduce the data volume to rates that can be analyzed and distributed in real time.
2. Based on a staring array, the HPA™ will permit longer integration times, resulting in higher signal-to-noise ratios. This will allow the system to operate in lower light and higher clutter regimes than other systems.

3. Because it is a framing system, it has no motion artifacts and can be used from unstable platforms, or handheld.
4. Because it a staring device, it can run at high framing rates, ideal for transient signals and rapidly occurring events.
5. It is significantly smaller and more robust than current technology, allowing for use on satellites, aircraft, robots, or handheld.
6. Its low cost will enable distributed systems in a given environment. Multiple systems will provide redundancy, insuring that essential data will be obtained regardless of individual instrument loss or failure.

ACKNOWLEDGEMENTS

Development of the HyperPixel Array™ technology was funded, in part, by the United States Government through the Air Force SBIR Program, the Navy and the Missile Defense Agency. Visible-NIR HPA instrument prototypes were demonstrated under contracts F19628-03-C-0079, W9113M-04-P-0073 and N00164-05-C-6077. The LWIR HPA instrument was developed and demonstrated under contract FA8718-04-C-0053. The MWIR HPA instrument was developed under contracts FA8718-05-C-0002 and FA8718-06-C-0063. The authors wish to express their appreciation to the Technical Monitors of these contracts for their contributions to the successful development of the HPA technology.

REFERENCES

[1] Green, R. O., B. Pavri, J. Faust, and O. Williams, "AVIRIS radiometric laboratory calibration, inflight validation, and a focused sensitivity analysis" in *Proceedings of the 8th JPL Airborne Earth Science Workshop*: NASA Jet Propulsion Laboratory, 1998. http://trs-new.jpl.nasa.gov/dspace/handle/2014/13692

[2] Basedow, R.W., Carmer, D.C., Anderson, M.E., "HYDICE System: Implementation and Performance", *Proc. SPIE*, **2480**, Imaging Spectrometry, Michael R. Descour; Jonathan M. Mooney; David L. Perry; Luanna R. Illing, Editors, pp.258-267, 1995.

[3] Vaughan, R.G., W.M. Calvin, and J.V. Taranik, "SEBASS hyperspectral thermal infrared data: Calibrated surface emissivity and mineral mapping", *Remote Sensing of Environment*, **85**, no. 1, pp. 48-63, 2003.

[4] ENVI geospatial processing software, a product of ITT Visual Information Systems, Boulder, CO.